

Sectional forces for seismic design of R/C frames by linear time history analysis and application to 3D single-story buildings

K.G. Kostinakis, A.M. Athanatopoulou*, I.E. Avramidis

Department of Civil Engineering, Aristotle University of Thessaloniki 54124, Thessaloniki, Greece

ARTICLE INFO

Article history:

Received 23 March 2010

Received in revised form

31 August 2010

Accepted 2 September 2010

ABSTRACT

The aim of the present paper is to present a rational procedure for the appropriate selection of the sectional forces needed for the calculation of the longitudinal reinforcement to R/C elements within the context of linear time history analysis. The proposed procedure is based on the maximum normal stresses, which occurs in each relevant cross section, and takes into consideration the critical angle of the seismic excitation, i.e., the angle that yields the maximum value of each response quantity of interest. Moreover, in an attempt to realistically interpret pertinent code provisions, three other code compatible methods of selecting the cross sectional forces are presented and compared to the here proposed method. For this purpose, three single-story buildings subjected to 47 bi-directional strong earthquake ground motions are analyzed. For each ground motion, the longitudinal reinforcement at all critical cross sections is calculated using the above four methods. Furthermore, the necessary reinforcement due to 3 and 7 representative earthquake records, required by the seismic code provisions, is determined. Comparison of results clearly shows that methods compatible with current seismic code provisions can significantly underestimate the necessary reinforcement with regards to the proposed method.

© 2010 Elsevier Ltd. All rights reserved.

1. Introduction

Modern seismic codes [1–5] suggest the linear time history analysis as one of the methods that can be used for the seismic analysis and design of R/C structures. According to this method, a spatial model of the structure is analyzed using simultaneously imposed consistent pairs of earthquake records along each of the two horizontal structural axes (N.b.: with a few exceptions, the vertical component of the ground motion is allowed to be ignored [2,3]). Then the maximum values of the action effects due to such bi-directional excitation, which are determined by time integration, are used to calculate the reinforcement at every relevant cross section.

The application of this method raises a series of questions regarding, among others, the choice of the excitation's incident angle and the proper (i.e., safe but not over the odds conservative) selection of the sectional forces required for the final design of the R/C structural elements, as code provisions are lacking the necessary explicitness with regard to these aspects.

An important issue, which has not yet been thoroughly studied, is the proper combination of the sectional forces required for the design of the R/C structural elements. For example, the determination of the longitudinal reinforcement of a column in a

3D frame depends on three response parameters: the axial force N and two bending moments (M_x , M_y) that act simultaneously. For such cases, seismic codes do not provide clear instructions for the proper combination of the values of the sectional forces needed for the calculation of the longitudinal reinforcement.

Another significant issue, closely related to the proper selection of the values of the frame's sectional forces required for the final design of the R/C frame elements, is the orientation of the two horizontal components of the ground motion, as it strongly affects the response quantities and, consequently, the reinforcement steel ratio. It is important to note that none of the seismic codes prescribes clearly the orientation of the horizontal axes along which the accelerograms should be applied; hence it is common practice to apply the horizontal seismic components along the so-called structural axes, i.e., the axes along which the earthquake resisting structural elements are arranged in plan-view. However, it is prudent to perform the seismic analysis for those orientations of seismic motion that yield the maximum response.

Several researchers [6–14] have investigated the critical seismic incident angle and the corresponding maximum response *within the context of response spectrum method*. Lopez et al. [10,13] proved that the critical value for a single response quantity can be up to 20% larger than the usual response produced, when the seismic components are applied along the structural axes. Menun and Der Kiureghian [11,12] and Anastassiadis et al. [14] determined the critical incident angle for the most unfavourable

* Corresponding author. Tel.: +30 2310 995837; fax: +30 2310 995679.
E-mail address: minak@civil.auth.gr (A.M. Athanatopoulou).

combinations of two or more simultaneous response parameters. In these studies, the excitation is described in terms of design spectra.

Besides, research has been conducted to determine the maximum response and the corresponding critical angle within the context of *linear time history analysis*. Fernandez-Davila et al. [15] have demonstrated that the maximum response in any structural element, due to bi-directional ground motion does not necessarily coincide with the response produced by accelerograms applied along the structural axes. Athanatopoulou [16] has developed analytical formulae for the determination of the critical angle of seismic incidence and the corresponding maximum value of any response quantity in structures subjected to two horizontal seismic components. The application of these formulae [16] to symmetric and asymmetric multistory buildings [16–18] has shown that the maximum value of a response quantity can be up to 180% larger than the response produced, when the seismic components act along the structural axes. Moreover it has been proved [16–18] that the same earthquake records have different critical angles for different response quantities. In spite of this evidence, in current practice, the components of the seismic motion are generally applied along the structural axes of the buildings.

The objective of the present paper is to present a rational procedure for the appropriate selection of the sectional forces needed for the calculation of the required longitudinal reinforcement in concrete frame elements within the context of linear time history analysis. The proposed method utilizes the simultaneous values of internal forces corresponding to the maximum normal stress at a cross section due to all possible seismic incident angles. Moreover, a numerical study is conducted in order to compare the results produced by the proposed method with the results produced by methods according to which the accelerograms are applied along the structural axes.

2. Review of code provisions

The aim of this section is to give an overview of code provisions regarding the orientation of horizontal seismic components and the selection of sectional forces within the context of the linear time history analysis. The reference codes are EC8 (Part 1) [1], NEHRP (FEMA450) [2], FEMA356 [3], ASCE 41/06 [4] and EAK2003 [5].

2.1. Orientation of seismic components

Concerning the angle of seismic incidence, FEMA356 and ASCE 41/06 state that the structural elements of the building “shall be designed for combinations of forces and deformations from separate analyses performed for ground motions in X and Y directions” (with a few exceptions, the vertical component of the ground motion is allowed to be ignored). However, it is not clearly defined how the orientation of X and Y axes should be chosen. It is also specified that the “30%-rule” will be used, in order to define the response quantities required for the final design of the structural elements. According to “30%-rule,” structural elements shall be designed for 100% of the maximum response, when the one component of the motion is applied along one horizontal direction plus 30% of the maximum response, when the other component of the ground motion is applied along the orthogonal direction. However, it is also stated that “alternatively, an analysis of a three-dimensional mathematical model, using simultaneously imposed consistent pairs of earthquake ground motion records along each of the horizontal axes of the building shall be permitted”.

Similarly, neither NEHRP nor EAK2003 defines the orientation of the excitation, whereas EC8 specifies that “the design seismic action shall be applied along all relevant horizontal directions and their orthogonal horizontal directions”. Yet, an explicit definition of the “relevant directions” is given only for a specific class of buildings: “for buildings with resisting elements in two perpendicular directions, these two directions shall be considered as the relevant directions”.

From the previous paragraphs, it becomes evident that none of the above seismic codes defines clearly the orientation of the axes along which the accelerograms should be applied; hence it is common practice to apply the components of the seismic motion along the structural axes of the buildings (if they exist).

2.2. Selection of sectional forces

Regarding the combination of sectional forces (axial force and two bending moments) which should be used for design purposes, none of the seismic codes defines which is the proper (i.e., safe but not too conservative) combination. EC8, NEHRP, FEMA356 and ASCE 41/06 specify that when three time history data sets are used as the seismic input, the maximum value of *each response parameter must be used for design*, while in case of seven or more time history data sets the average value of each response parameter may be permitted to determine design acceptability. We see that codes do not clarify which is the response parameter: each individual sectional force (moment) or normal stress (which is composed of a component attributable to axial force and two components attributable to bending moments).

3. Critical orientation and maximum response

The earthquake-induced translational motion at a specific point of the ground is recorded along the two horizontal directions and one vertical. However, with a few exceptions, the vertical component of the ground motion is allowed to be ignored. Assume a structure, which is subjected to bidirectional horizontal seismic motion, represented by the recorded accelerograms $\alpha_x(t)$ and $\alpha_y(t)$ along the orthogonal axes p and w . As the direction of the seismic motion is unknown, the axes p and w can form any angle θ^s with respect to the structural axes X and Y , respectively (Fig. 1a). Clearly, the structural response is a function of the seismic incident angle θ^s . Each response parameter R attains its maximum value $\max R$ for a specific seismic incident angle θ_{cr1} (Fig. 1a). The maximum value $\max R$ and the corresponding critical angle θ_{cr1} are computed according to the following procedure [16]:

- Compute the response due to excitation ‘ $\alpha 0^\circ$ ’ (Fig. 1b). The accelerograms $\alpha_x(t)$ and $\alpha_y(t)$ are applied simultaneously along axes X and Y , respectively, i.e., the angle of seismic incidence is $\theta^s = 0^\circ$. A typical response quantity is denoted as $R_{,\alpha 0}$.
- Compute the response due to excitation ‘ $\alpha 90^\circ$ ’ (Fig. 1c). The accelerograms $\alpha_x(t)$ and $\alpha_y(t)$ are applied simultaneously along axes Y and X , respectively, i.e., the angle of seismic incidence is $\theta^s = 90^\circ$. A typical response quantity is denoted as $R_{,\alpha 90}$.
- The maximum value of a response parameter for any angle θ^s of seismic incidence is given as a function of time by Eq. (1) [16]

$$R_0(t) = [R_{,\alpha 0}^2(t) + R_{,\alpha 90}^2(t)]^{1/2} \quad (1)$$

The plot of the function $\pm R_0(t)$ provides the maximum/minimum value of the required response parameter as well as the

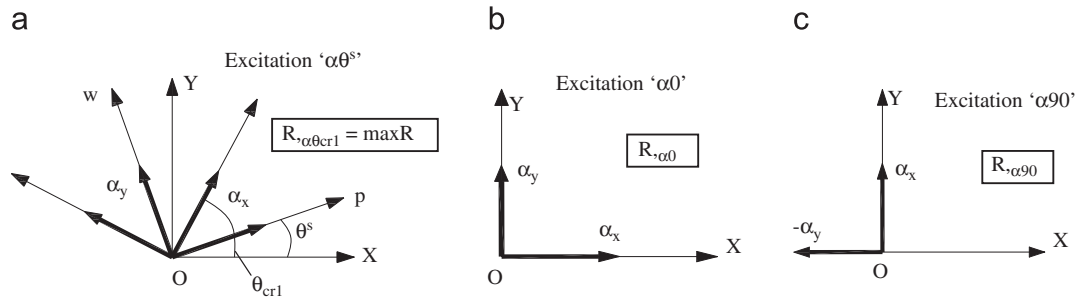


Fig. 1. Excitations ' $\alpha\theta^s$ ', ' $\alpha 0$ ' and ' $\alpha 90$ '.

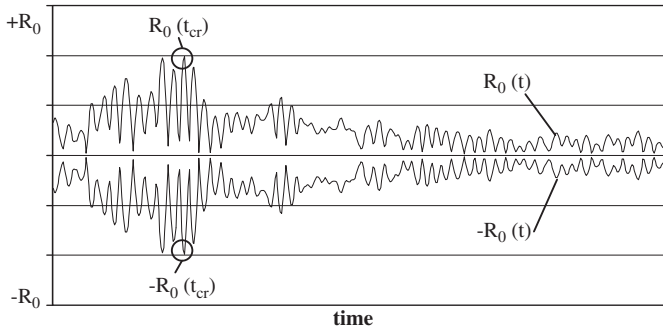


Fig. 2. Responses $R_0(t)$ and $-R_0(t)$.

time instant t_{cr} at which this maximum/minimum occurs (Fig. 2)
 $\max R = +R_0(t_{cr}), \quad \min R = -R_0(t_{cr})$ (2)

The corresponding critical angles θ_{cr1} (maximum value) and θ_{cr2} (minimum value) are given by Eq. (3)

$$\theta_{cr1} = \tan^{-1} \left(\frac{R_{,z90}(t_{cr})}{R_{,z0}(t_{cr})} \right), \quad \theta_{cr2} = \theta_{cr1} - \pi$$
 (3)

It must be noted that the maximum value $\max R$ is computed without the previous determination of angle θ_{cr1} . Moreover the value of any response parameter, R , due to seismic motion ' $\alpha\theta^s$ ' can be computed by the following equation [16]:

$$R_{,\alpha\theta^s}(t) = R_{,z0}(t) \cos \theta^s + R_{,z90}(t) \sin \theta^s$$
 (4)

4. Methods of selecting the sectional forces

In the present section, four methods of selecting the set of sectional forces needed for the calculation of the longitudinal reinforcement in concrete frame elements within the context of linear time history analysis are presented. The first method is proposed by the authors, since it is considered as the most rational. According to this method, the maximum axial stresses at any relevant cross section due to any orientation of the ground motion are used in order to determine the combinations of the sectional forces required for the design of the structural elements. The use of the axial stresses has already been used for the design of R/C elements within the context of the response spectrum method [7,14,19], since they were considered as the only quantity that adequately captures the response of a frame section under the simultaneous action of axial force and bending moments.

In an attempt to interpret the pertinent seismic code provisions, three other methods of selecting the sectional forces are introduced. According to these methods, the earthquake

components are applied along the structural axes as seismic codes suggest. In the following subsections, the four methods of selecting the sectional forces in R/C frame elements are presented.

4.1. Method of extreme stresses (MS_{ex})

This method (denoted in the following as MS_{ex}) is proposed by the authors as the most rational, because it is based on the simultaneous values of sectional forces corresponding to the maximum/minimum value of normal stresses occurred at a frame section for any angle of the seismic incidence. The steps of the method are as follows:

- Two time history loading cases are performed due to bi-directional earthquake motion. The first one due to excitation " $\alpha 0$ " ($\theta^s = 0^\circ$) and the second one due to excitation " $\alpha 90$ " ($\theta^s = 90^\circ$) (Fig. 1). The time histories of the response parameters of interest $N(t)_{,\alpha 0}$, $M_{\xi}(t)_{,\alpha 0}$ and $M_{\eta}(t)_{,\alpha 0}$ as well as $N(t)_{,\alpha 90}$, $M_{\xi}(t)_{,\alpha 90}$ and $M_{\eta}(t)_{,\alpha 90}$ (the symbol ' $\alpha 0$ ' or ' $\alpha 90$ ' after the comma denotes due to excitation ' $\alpha 0$ ' or ' $\alpha 90$ ', respectively) are computed.
- The time histories of the axial stresses at the four corners of a rectangular cross section, $\sigma_{k,\alpha 0}(t)$ and $\sigma_{k,\alpha 90}(t)$ ($k=A, B, C, D$) (Fig. 3) due to excitation ' $\alpha 0$ ' and ' $\alpha 90$ ', respectively, are computed

$$\sigma_{k,\alpha 0}(t) = \frac{N_{,\alpha 0}(t)}{A} - \frac{a}{2} \frac{M_{\eta,\alpha 0}(t)}{I_{\eta}} + \frac{b}{2} \frac{M_{\xi,\alpha 0}(t)}{I_{\xi}}$$
 (5)

$$\sigma_{k,\alpha 90}(t) = \frac{N_{,\alpha 90}(t)}{A} - \frac{a}{2} \frac{M_{\eta,\alpha 90}(t)}{I_{\eta}} + \frac{b}{2} \frac{M_{\xi,\alpha 90}(t)}{I_{\xi}}$$
 (6)

The reference system and the positive sectional forces are shown in Fig. 3.

- Using Eq. (1), the function $\sigma_{0k}(t)$ (Eq. (1)) is computed

$$\sigma_{0k}(t) = [\sigma_{k,\alpha 0}^2(t) + \sigma_{k,\alpha 90}^2(t)]^{1/2}$$
 (7)

- Plot the function $\sigma_{0k}(t)$ and determine the time instant, t_{cr} , as well as the associated maximum and minimum values $\pm \sigma_{0k}(t_{cr})$ at the corner k .
- The critical seismic incident angles are computed, using Eq. (3)

$$\theta_{cr1} = \tan^{-1} \left(\frac{\sigma_{k,\alpha 90}(t_{cr})}{\sigma_{k,\alpha 0}(t_{cr})} \right) \text{ and } \theta_{cr2} = \theta_{cr1} - \pi$$
 (8)

- The values of the sectional forces due to excitation ' $\alpha 0$ ' and ' $\alpha 90$ ' at the time instant, t , are known (step 1). Therefore the values of the sectional forces at the time instant, t_{cr} , that correspond to the seismic incident angle, θ_{cri} ($i=1,2$), are computed, using Eq. (4)

$$R'(\theta_{cri}, t) = R'_{,\alpha 0}(t_{cr}) \cos \theta_{cri} + R'_{,\alpha 90}(t_{cr}) \sin \theta_{cri}$$

where R' is N , M_{ξ} and M_{η} .

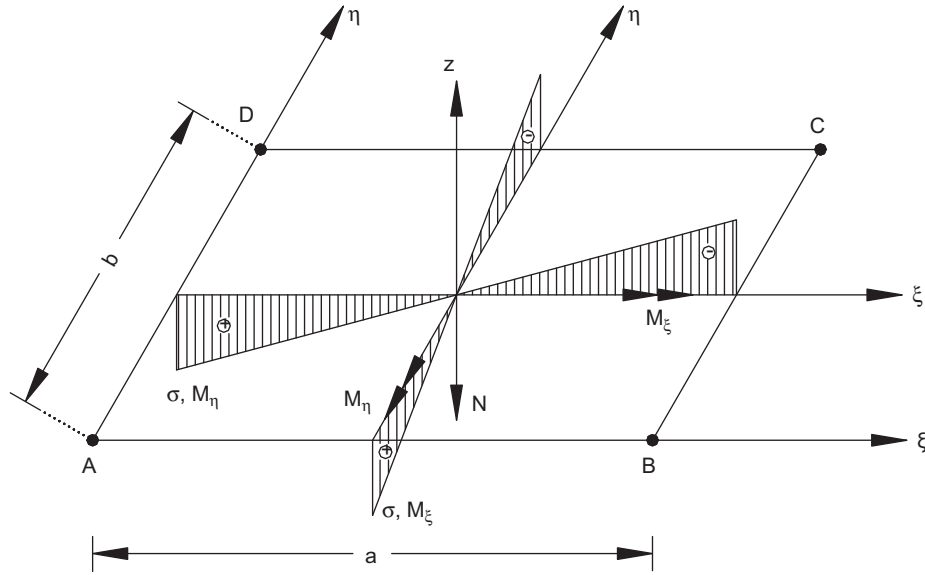


Fig. 3. Local reference system of a cross section showing sectional forces and normal stresses.

Table 1
Design combinations for method MS_{ex} .

$\max \sigma_A$	$N, \max \sigma_A$	$M_\xi, \max \sigma_A$	$M_\eta, \max \sigma_A$
$\min \sigma_A$	$N, \min \sigma_A$	$M_\xi, \min \sigma_A$	$M_\eta, \min \sigma_A$
$\max \sigma_B$	$N, \max \sigma_B$	$M_\xi, \max \sigma_B$	$M_\eta, \max \sigma_B$
$\min \sigma_B$	$N, \min \sigma_B$	$M_\xi, \min \sigma_B$	$M_\eta, \min \sigma_B$
$\max \sigma_C$	$N, \max \sigma_C$	$M_\xi, \max \sigma_C$	$M_\eta, \max \sigma_C$
$\min \sigma_C$	$N, \min \sigma_C$	$M_\xi, \min \sigma_C$	$M_\eta, \min \sigma_C$
$\max \sigma_D$	$N, \max \sigma_D$	$M_\xi, \max \sigma_D$	$M_\eta, \max \sigma_D$
$\min \sigma_D$	$N, \min \sigma_D$	$M_\xi, \min \sigma_D$	$M_\eta, \min \sigma_D$

These values correspond to the maximum stress, $+\sigma_k$ and minimum stress, $-\sigma_k$. Therefore, they are considered as an unfavourable combination of simultaneous sectional forces ($N(t_{cr}, \theta_{cr1}), M_\xi(t_{cr}, \theta_{cr1}), M_\eta(t_{cr}, \theta_{cr1})$) and ($N(t_{cr}, \theta_{cr2}), M_\xi(t_{cr}, \theta_{cr2}), M_\eta(t_{cr}, \theta_{cr2})$). For the four corners of a rectangular cross section, a total number of eight unfavourable combinations (four for the positive (tension) sign and four for the negative (compression) sign of σ) results.

In Table 1, the eight unfavourable combinations produced by the proposed method are presented (the term after comma denotes corresponding to). These are the most unfavourable combinations of sectional forces due to seismic loads. Then, the effects of the vertical and the seismic loads are added and the final unfavourable design combinations of the sectional forces are obtained. These combinations are used for the calculation of the required longitudinal reinforcement areas. Finally, the maximum value of the 8 steel areas is selected as the required one.

4.2. Method of maximum absolute forces for angle $\alpha=0^\circ$ (MF_{abs0})

According to this method (denoted in the following as MF_{abs0}), the acceleration loads $\alpha_x(t)$ and $\alpha_y(t)$ are applied simultaneously along the structural axes X and Y, respectively, (excitation ‘ $\alpha 0$ ’) (Fig. 1b) as codes specify. The design procedure according to this method is as follows:

1. One time history loading case due to excitation ‘ $\alpha 0$ ’ is performed and the time history of any response parameter ($N(t)_{\alpha 0}, M_\xi(t)_{\alpha 0}$ and $M_\eta(t)_{\alpha 0}$) is computed.

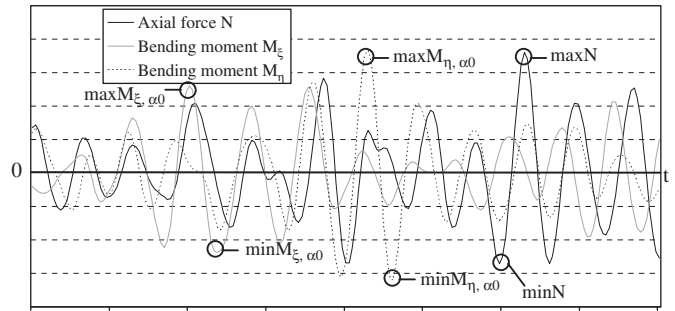


Fig. 4. Curves $N(t)_{\alpha 0}, M_\xi(t)_{\alpha 0}$ and $M_\eta(t)_{\alpha 0}$.

Table 2
Design combinations for the method MF_{abs0} .

$\max N_{\alpha 0} $	$\max M_{\xi \alpha 0} $	$\max M_{\eta \alpha 0} $
$\max N_{\alpha 0}$	$\max M_{\xi \alpha 0}$	$-\max M_{\eta \alpha 0} $
$\max N_{\alpha 0}$	$-\max M_{\xi \alpha 0} $	$\max M_{\eta \alpha 0} $
$\max N_{\alpha 0} $	$-\max M_{\xi \alpha 0}$	$-\max M_{\eta \alpha 0} $
$-\max N_{\alpha 0}$	$\max M_{\xi \alpha 0} $	$\max M_{\eta \alpha 0} $
$-\max N_{\alpha 0} $	$\max M_{\xi \alpha 0}$	$-\max M_{\eta \alpha 0} $
$-\max N_{\alpha 0}$	$-\max M_{\xi \alpha 0} $	$\max M_{\eta \alpha 0} $
$-\max N_{\alpha 0} $	$-\max M_{\xi \alpha 0}$	$-\max M_{\eta \alpha 0} $

2. The maximum/minimum values of the response parameters $N(t)_{\alpha 0}, M_\xi(t)_{\alpha 0}$ and $M_\eta(t)_{\alpha 0}$ are determined (Fig. 4). The maximum absolute (no simultaneous) values of these response parameters are used for design purposes.

The sign of each parameter can be positive or negative. Any combination of these values can be considered as an unfavourable combination of the sectional forces. Hence, the eight unfavourable combinations of sectional forces presented in Table 2 are produced.

These are the most unfavourable combinations of sectional forces due to seismic loads. Then, the effects of the vertical and the seismic loads are added and the final unfavourable design combinations of the sectional forces are obtained. These combinations are used for the calculation of the required longitudinal reinforcement areas. Finally, the maximum value of the 8 steel areas is selected as the required one.

4.3. Method based on the 30% combination Rule (M30)

This method (denoted in the following as M30) stems from FEMA/356 and ASCE/41-06 provisions. The steps of the method are as follows:

1. A time history loading case due to uni-directional excitation with the accelerogram $\alpha_x(t)$ applied along the X-axis, is performed and the time histories of the response parameters $N(t)_{,x}$, $M_\xi(t)_{,x}$ and $M_\eta(t)_{,x}$ are computed. Then, the maximum absolute value of each parameter is determined (Fig. 5a).
2. A time history loading case due to uni-directional excitation with the accelerogram $\alpha_y(t)$ applied along the Y-axis is performed and the time histories of the response parameters $N(t)_{,y}$, $M_\xi(t)_{,y}$ and $M_\eta(t)_{,y}$ are computed. Then, the maximum absolute value of each parameter is determined (Fig. 5b).

3. The maximum value of each response parameter is calculated using the 30% combination rule [3,4].

$$\max R = \pm \max |R_{,x}| \pm 0.30 \max |R_{,y}|$$

$$\max R = \pm 0.30 \max |R_{,x}| \pm \max |R_{,y}|$$

where R : N , M_ξ and M_η

The sets of sectional forces for design purposes, according to this method, for any relevant cross section, are presented in Table 3.

These are the most unfavourable combinations of sectional forces due to seismic loads. Then, the effects of the vertical and the seismic loads are added, and the final unfavourable design combinations of the sectional forces are obtained. These combinations are used for the calculation of the required longitudinal reinforcement areas. Finally, the maximum value of the 8 steel areas is selected as the required one.

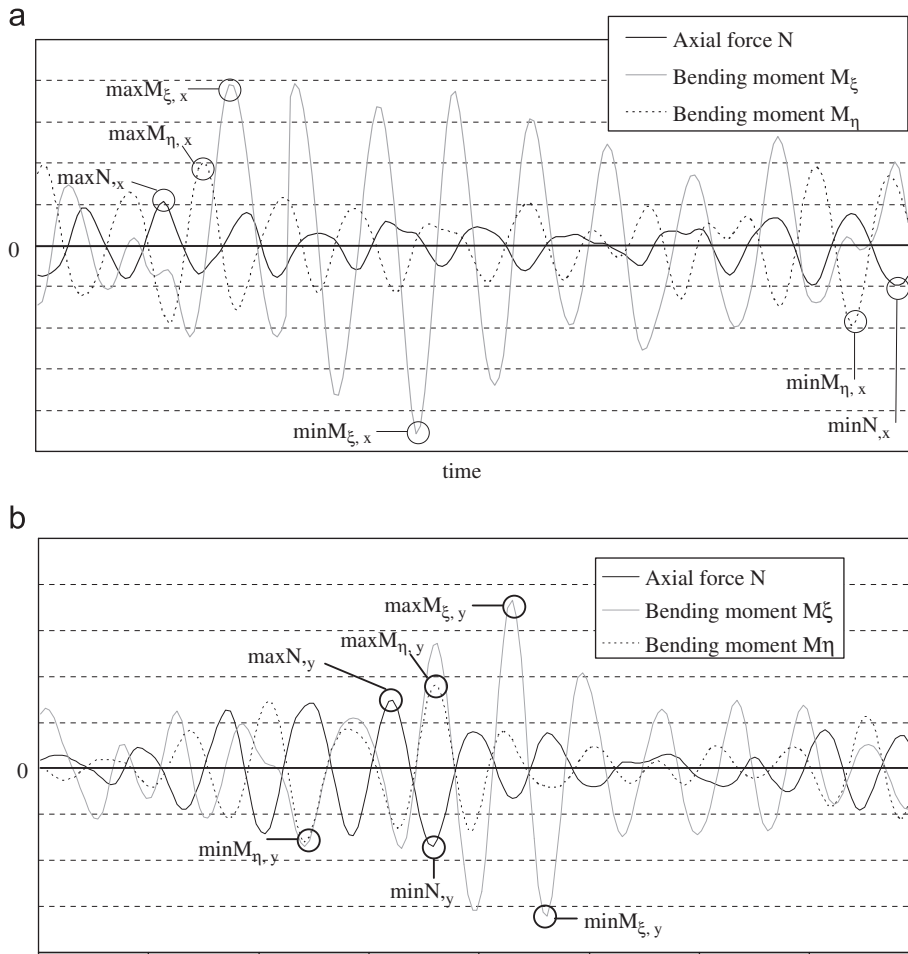


Fig. 5. Time histories of response parameters $N(t)_{,i}$, $M_\xi(t)_{,i}$ and $M_\eta(t)_{,i}$ ((a) $i=x$ and (b) $i=y$).

Table 3
Design combinations for the method M30.

$\max N_{,x} + 0.3 \max N_{,y} $	$\max M_{\xi,x} + 0.3 \max M_{\xi,y} $	$\max M_{\eta,x} + 0.3 \max M_{\eta,y} $
$\max N_{,x} - 0.3 \max N_{,y} $	$\max M_{\xi,x} - 0.3 \max M_{\xi,y} $	$\max M_{\eta,x} - 0.3 \max M_{\eta,y} $
$-\max N_{,x} + 0.3 \max N_{,y} $	$-\max M_{\xi,x} + 0.3 \max M_{\xi,y} $	$-\max M_{\eta,x} + 0.3 \max M_{\eta,y} $
$-\max N_{,x} - 0.3 \max N_{,y} $	$-\max M_{\xi,x} - 0.3 \max M_{\xi,y} $	$-\max M_{\eta,x} - 0.3 \max M_{\eta,y} $
$0.3 \max N_{,x} + \max N_{,y} $	$0.3 \max M_{\xi,x} + \max M_{\xi,y} $	$0.3 \max M_{\eta,x} + \max M_{\eta,y} $
$0.3 \max N_{,x} - \max N_{,y} $	$0.3 \max M_{\xi,x} - \max M_{\xi,y} $	$0.3 \max M_{\eta,x} - \max M_{\eta,y} $
$-0.3 \max N_{,x} + \max N_{,y} $	$-0.3 \max M_{\xi,x} + \max M_{\xi,y} $	$-0.3 \max M_{\eta,x} + \max M_{\eta,y} $
$-0.3 \max N_{,x} - \max N_{,y} $	$-0.3 \max M_{\xi,x} - \max M_{\xi,y} $	$-0.3 \max M_{\eta,x} - \max M_{\eta,y} $

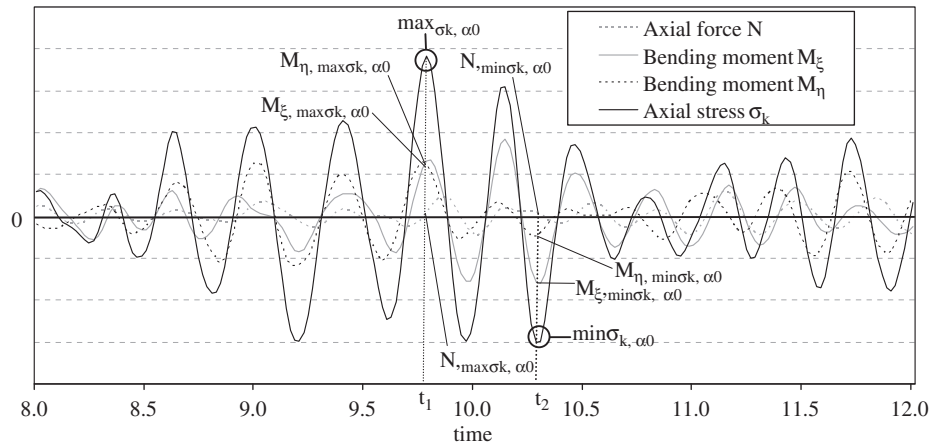


Fig. 6. Time histories of the response parameters $N(t)_{z0}$, $M_{\xi}(t)_{z0}$, $M_{\eta}(t)_{z0}$ and $\sigma_k(t)_{z0}$.

Table 4
Design combinations for method MS_{ex0} .

$\max_{\sigma A, z0}$	$N_{, \max \sigma A, z0}$	$M_{\xi, \max \sigma A, z0}$	$M_{\eta, \max \sigma A, z0}$
$\min_{\sigma A, z0}$	$N_{, \min \sigma A, z0}$	$M_{\xi, \min \sigma A, z0}$	$M_{\eta, \min \sigma A, z0}$
$\max_{\sigma B, z0}$	$N_{, \max \sigma B, z0}$	$M_{\xi, \max \sigma B, z0}$	$M_{\eta, \max \sigma B, z0}$
$\min_{\sigma B, z0}$	$N_{, \min \sigma B, z0}$	$M_{\xi, \min \sigma B, z0}$	$M_{\eta, \min \sigma B, z0}$
$\max_{\sigma C, z0}$	$N_{, \max \sigma C, z0}$	$M_{\xi, \max \sigma C, z0}$	$M_{\eta, \max \sigma C, z0}$
$\min_{\sigma C, z0}$	$N_{, \min \sigma C, z0}$	$M_{\xi, \min \sigma C, z0}$	$M_{\eta, \min \sigma C, z0}$
$\max_{\sigma D, z0}$	$N_{, \max \sigma D, z0}$	$M_{\xi, \max \sigma D, z0}$	$M_{\eta, \max \sigma D, z0}$
$\min_{\sigma D, z0}$	$N_{, \min \sigma D, z0}$	$M_{\xi, \min \sigma D, z0}$	$M_{\eta, \min \sigma D, z0}$

4.4. Method of extreme stresses for angle $\alpha=0^\circ$ (MS_{ex0})

According to this method (denoted in the following as MS_{ex0}), the acceleration loads $\alpha_x(t)$ and $\alpha_y(t)$ are applied simultaneously along the structural axes X and Y, respectively, (excitation ‘ $\alpha 0$ ’) (Fig. 1b) as codes specify. The steps of the method are as follows:

1. One time history loading case due to excitation ‘ $\alpha 0$ ’ is performed and the time history of any response parameter ($N(t)_{z0}$, $M_{\xi}(t)_{z0}$ and $M_{\eta}(t)_{z0}$) is computed.
2. The time history of the normal stress at each corner of any rectangular cross section, $\sigma_{k,z0}$ ($k=A, B, C, D$), is computed (Eq. (5)) and plotted (Fig. 6). Hence, the maximum and minimum value of the axial stress as well as the corresponding time instants t_1 and t_2 , respectively, are determined (Fig. 6).
3. The sectional forces $N(t_j)_{z0}$, $M_{\xi}(t_j)_{z0}$ and $M_{\eta}(t_j)_{z0}$ ($j=1,2$) that correspond to time instants t_1 and t_2 are known (step 1). These are considered as unfavourable combinations of sectional forces and are used for the design.

Two unfavourable combinations, for each corner of a rectangular section, are produced (one for the maximum axial stress and one for the minimum axial stress). Hence, for the four corners of the considered section, the eight unfavourable combinations shown in Table 4 are produced.

These are the unfavourable combinations due to seismic loads. Then, the effects of the vertical and the seismic loads are added and the final unfavourable design combinations of the sectional forces are obtained. These combinations are used for the calculation of the required longitudinal reinforcement areas. Finally, the maximum value of the 8 steel areas is selected as the required one.

5. Structural models

Three structural models are considered in this study. Each model represents a single-story reinforced concrete building. The deck is considered to be absolutely rigid in-plan, square in shape ($L=B=11$ m) and it is supported by four parallel plane frames in each direction (Fig. 7). The height of the story is 4.5 m. The concrete strength and the yield strength of the reinforcing steel are 20 and 500 MPa, respectively. The modulus of elasticity is taken equal to $E=29$ GPa and the damping ratio is assumed to be $\zeta=5\%$, for all the modes of vibration.

The cross sectional dimensions of beams and columns are 20/50 (cm) and 30/30 (cm), respectively. The first model is a torsionally balanced system ($E_s=0$, E_s is the structural eccentricity). For each one of the other two models, it is considered that the Mass Centre CM is located on the X-axis at a distance, E_s , from the Rigidity Centre CR. Regarding the structural eccentricity, two values were chosen: $e_s=E_s/L=0.1$ and $e_s=E_s/L=0.2$. The three vibration periods of the buildings considered in the present study are shown in Fig. 7.

It is important to notice that the methods presented in the previous paragraphs can be applied to any R/C building. However, the application of the aforementioned methods to multi-story buildings requires huge computational effort, as they are not implemented in an existing design software. It is interesting to mention that, for the three single-story buildings studied in the present paper, the longitudinal reinforcement corresponding to a total of 239,136 combinations of sectional forces had to be calculated.

6. Ground motions

Forty seven (47) pairs of horizontal ground motion records obtained from the PEER strong motion database (<http://peer.berkeley.edu/smcat/>) have been used as an input ground motion for the analyses of the buildings presented in the previous section. The ground motions, which are chosen with the aid of the Appendix C of FEMA 440 [20], have magnitudes (M_s) between 6.0 and 7.4 and are not characterized by forward-directivity effects. Additional information regarding the ground motions can be found in [21]. The motions are classified into two groups: a group of 28 ground motions (Table 5) recorded on Soil type A according to the classification of the Greek Seismic Code (soil types B and C of FEMA356) and a group of 19 ground motions (Table 6) recorded on Soil type B according to the classification of the same Code (soil type D of FEMA356).

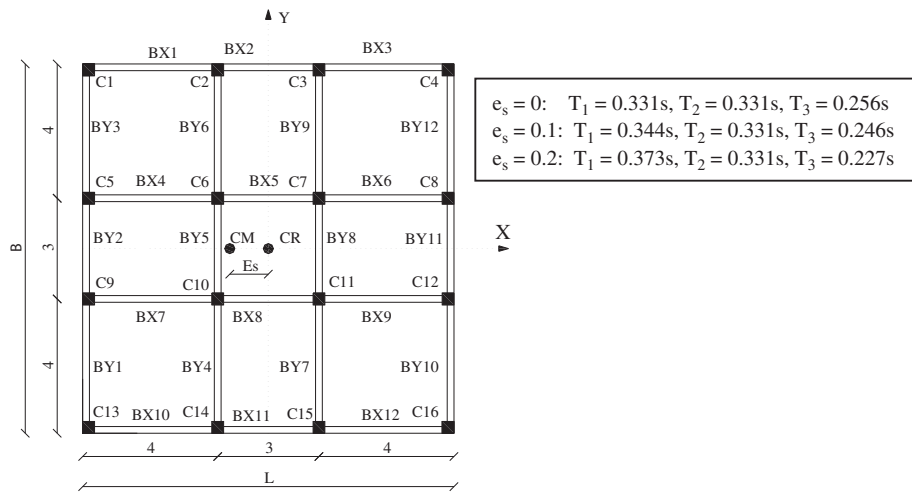


Fig. 7. Structural model (CM: mass centre; CR: rigidity centre) and vibration periods.

Table 5
Ground motions recorded on soil type A of the Greek Seismic Code.

No.	Date	Earthquake name	Magnitude (Ms)	Station name	Station number	Closest distance to fault rupture (Km)	Component (deg.)	PGA (g)
1	28/6/1992	Landers	7.4	Silent Valley, Poppet Flat	12,206	51.7	0	0.050
2	28/6/1992	Landers	7.4	Twenty nine Palms Park Maintainance Building	22,161	42.2	0	0.080
3	28/6/1992	Landers	7.4	Amboy	21,081	69.2	90	0.060
4	18/10/1989	Loma Prieta	7.1	Point Bonita	58,043	88.6	0	0.115
5	18/10/1989	Loma Prieta	7.1	Piedmont, Piedmont Jr. High Grounds	58,338	78.3	207	0.146
6	18/10/1989	Loma Prieta	7.1	San Francisco, Pacific Heights	58,131	81.6	297	0.071
7	18/10/1989	Loma Prieta	7.1	San Francisco, Rincon Hill	58,151	79.7	315	0.072
8	18/10/1989	Loma Prieta	7.1	San Francisco, Golden Gate Bridge	1678	85.1	45	0.084
9	18/10/1989	Loma Prieta	7.1	Hollister-SAGO vault	1032	30.6	270	0.061
10	18/10/1989	Loma Prieta	7.1	South San Francisco, Sierra Point	58,539	68.2	360	0.047
11	18/10/1989	Loma Prieta	7.1	Berkeley, Lawrence Berkeley Laboratory	58,471	83.6	0	0.078
12	18/10/1989	Loma Prieta	7.1	Coyote Lake Dam, Downstream	57,504	22.3	90	0.092
13	17/1/1994	Northridge	6.7	Mt. Wilson, CIT Seismic Station	24,399	36.1	270	0.233
14	17/1/1994	Northridge	6.7	Antelope Buttes	24,310	47.3	360	0.123
15	17/1/1994	Northridge	6.7	Los Angeles, Wonderland	90,017	22.7	270	0.036
16	17/1/1994	Northridge	6.7	Wrightwood, Jackson Flat	23,590	68.4	360	0.060
17	17/1/1994	Northridge	6.7	Littlerock-Brainard Can	23,595	46.9	115	0.056
18	17/1/1994	Northridge	6.7	San Gabriel, E. Grand Avenue	90,019	41.7	205	0.105
19	15/10/1979	Imperial Valley	6.9	Superstition Mountain	286	26.0	0	0.057
20	8/7/1986	N. Palm Springs	6.0	Anza-Red Mountain	5224	45.6	90	0.117
21	15/10/1979	Imperial Valley	6.9	El Centro, Parachute Test Facility	5051	14.2	195	0.160
22	9/2/1971	San Fernando	6.6	Pasadena, CIT Athenaeum	80,053	31.7	285	0.179
23	9/2/1971	San Fernando	6.6	Pearblossom Pump	269	38.9	0	0.234

Table 5 (continued)

No.	Date	Earthquake name	Magnitude (Ms)	Station name	Station number	Closest distance to fault rupture (Km)	Component (deg.)	PGA (g)
24	28/6/1992	Landers	7.4	Yermo, Fire Station	12,149	23.2	0	0.102
							0	0.171
							90	0.154
25	18/10/1989	Loma Prieta	7.1	Saratoga, Aloha Avenue	58,065	13.0	0	0.512
							90	0.324
26	18/10/1989	Loma Prieta	7.1	Gilroy, Gavilon College Phys Sch Building	47,006	11.6	337	0.325
							67	0.357
							0	0.450
27	18/10/1989	Loma Prieta	7.1	Santa Cruz, University of California	58,135	17.9	0	0.450
							90	0.395
28	18/10/1989	Loma Prieta	7.1	San Francisco, Dimond Heights	58,130	77.0	0	0.098
							90	0.113

Table 6

Ground motions recorded on soil type B of the Greek Seismic Code.

No.	Date	Earthquake name	Magnitude (Ms)	Station name	Station number	Closest distance to fault rupture (Km)	Component (deg)	PGA (g)
1	28/6/1992	Landers	7.4	Yermo, Fire Station	22,074	24.9	270	0.245
							360	0.152
2	28/6/1992	Landers	7.4	Palm Springs, Airport	12,025	37.5	0	0.076
							90	0.089
3	28/6/1992	Landers	7.4	Pomona, 4th and Locust, Free Field	23,525	117.0	0	0.067
							90	0.044
4	17/1/1994	Northridge	6.7	Los Angeles, Hollywood Storage Bldg.	24,303	25.5	360	0.358
							90	0.231
5	17/1/1994	Northridge	6.7	Santa Monica City Hall	24,538	27.6	360	0.370
							90	0.883
6	17/1/1994	Northridge	6.7	Los Angeles, N. Westmoreland	90,021	29.0	270	0.361
							0	0.401
7	18/10/1989	Loma Prieta	7.1	Gilroy #2, Hwy 101 Bolsa Road Motel	47,380	12.7	0	0.367
							90	0.322
8	18/10/1989	Loma Prieta	7.1	Gilroy #3, Sewage Treatment Plant	47,381	14.4	0	0.555
							90	0.367
9	18/10/1989	Loma Prieta	7.1	Hayward, John Muir School	58,393	57.4	0	0.171
							90	0.139
10	18/10/1989	Loma Prieta	7.1	Agnews, Agnews State Hospital	57,066	28.2	0	0.172
							90	0.159
11	10/1/1987	Whittier Narrows	5.7	Los Angeles, 116th St. School	14,403	22.5	270	0.294
							360	0.396
12	10/1/1987	Whittier Narrows	5.7	Downey, Country Maintenance Building	14,368	18.3	180	0.221
							270	0.141
13	15/10/1979	Imperial Valley	6.9	El Centro #13, Strobel Residence	5059	21.9	140	0.117
							230	0.139
14	15/10/1979	Imperial Valley	6.9	Calexico, Fire Station	5053	10.6	225	0.275
							315	0.202
15	24/4/1984	Morgan Hill	6.1	Gilroy #4, 2905 Anderson Road	57,382	12.8	270	0.224
							360	0.348
16	24/4/1984	Morgan Hill	6.1	Gilroy #7, Mantnilli Ranch, Jamison Road	57,425	14.0	0	0.190
							90	0.113
17	24/4/1984	Morgan Hill	6.1	Gilroy #2, Keystone Road	47,380	15.1	0	0.162
							90	0.212
18	24/4/1984	Morgan Hill	6.1	Gilroy #3, Sewage Treatment Plant	47,381	14.6	0	0.194
							90	0.200
19	9/2/1971	San Fernando	6.6	Los Angeles, Hollywood Storage Building	135	21.2	90	0.210
							180	0.174

The accelerograms of each group were scaled, so as to match the design spectrum of the Greek Seismic Code [5] for Peak Ground Acceleration, $PGA=0.36\text{ g}$ and behavior factor $q=3.5$. The two design spectra for soil types A and B are shown in Fig. 8 (solid black line). The accelerograms were scaled to the corresponding design spectrum, according to the procedure suggested by FEMA356 [3]. That is, each pair of accelerograms was scaled such that the SRSS of the 5%-damped site-specific spectrum of the scaled horizontal components does not fall below 1.4 times the 5%-damped design spectrum for periods

between 0.2 T and 1.5 T (where T is the fundamental period of the building).

7. Comparative assessment of numerical results

7.1. Individual ground motions

Each one of the three models, considered in the present study, was analyzed using the SAP2000 [22] for the vertical as well as

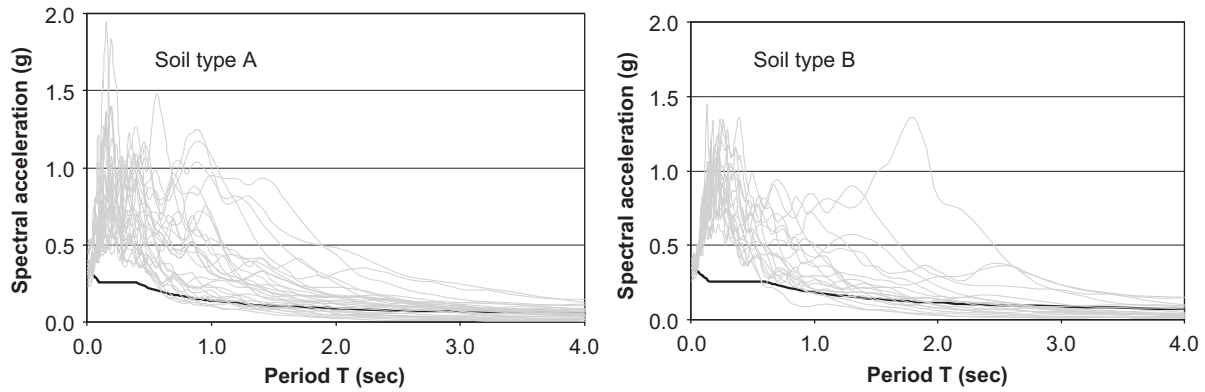


Fig. 8. SRSS of the 5%-damped spectra of the scaled accelerograms for the torsionally balanced system (grey lines). Black line corresponds to the design spectrum of the Greek Seismic Code.

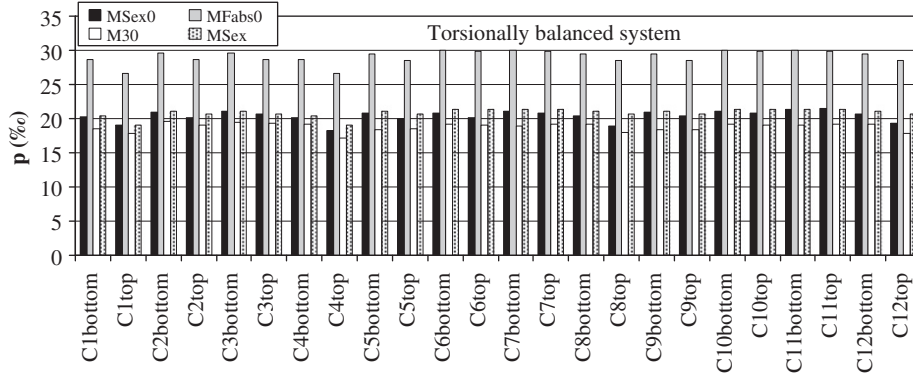


Fig. 9. Reinforcement steel ratios (p) of the columns for the torsionally balanced system under “Loma Prieta” earthquake (No. 6 of Table 5).

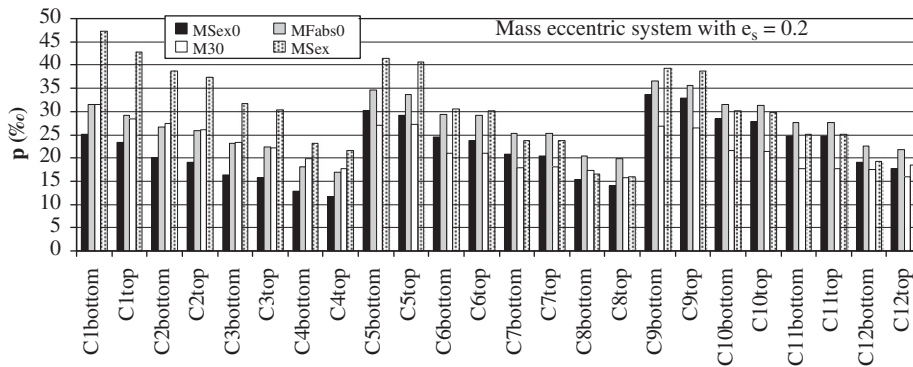


Fig. 10. Reinforcement steel ratios (p) of the columns for the mass eccentric system ($e_s=0.2$) under “Loma Prieta” earthquake (No. 6 of Table 5).

the seismic loads. Seismic loads are represented by the two horizontal components of each ground motion shown in Tables 5 and 6. For each ground motion, the longitudinal reinforcement steel ratios at every cross section of the buildings were calculated, using the combinations of sectional forces produced by the four methods described in Section 4. The reinforcement was computed according to the Greek Code for the Design and Construction of Concrete Works [23]. The constitutive laws adopted for steel and concrete are those suggested by the Eurocode 2 [24] and by CEB-FIB [25]. The axial load-bending moment interaction diagrams are those constructed by CEB, 1982 [26].

The reinforcement steel ratios for every critical cross section of the columns under “Loma Prieta” earthquake (soil type A) and “San Fernando” earthquake (soil type B) are presented in

Figs. 9–12. From these figures, it can be seen that the required reinforcement is significantly affected by the method used to select the design sectional forces in frame elements. Method MF_{abs0} produced the most conservative results for the torsionally balanced system, whereas for the mass eccentric system it is not clear which method leads to the largest longitudinal reinforcement steel ratios.

The reinforcement steel area calculated by the proposed method, MS_{ex} , is larger than the one computed by method MS_{ex0} . The difference between the two methods depends on the structural element, the earthquake record and the mass eccentricity of the building. For example, in the torsionally balanced system under “Loma Prieta” earthquake (Fig. 9), the aforementioned difference for the majority of the columns is negligible.

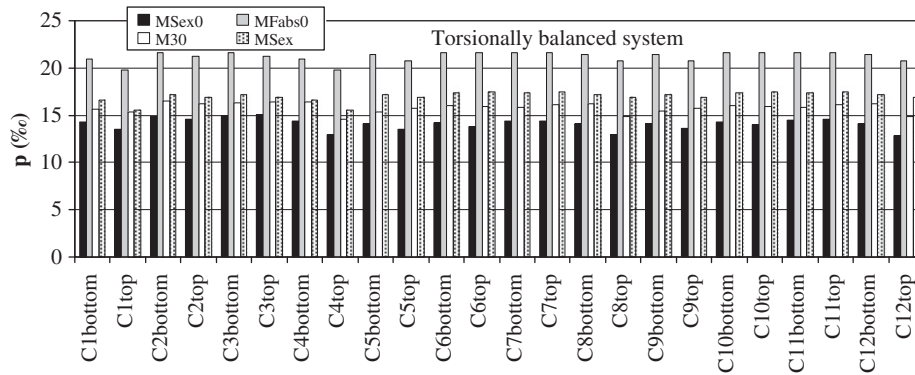


Fig. 11. Reinforcement steel ratios (p) of the columns for the torsionally balanced system under “San Fernando” earthquake (No. 19 of Table 6).

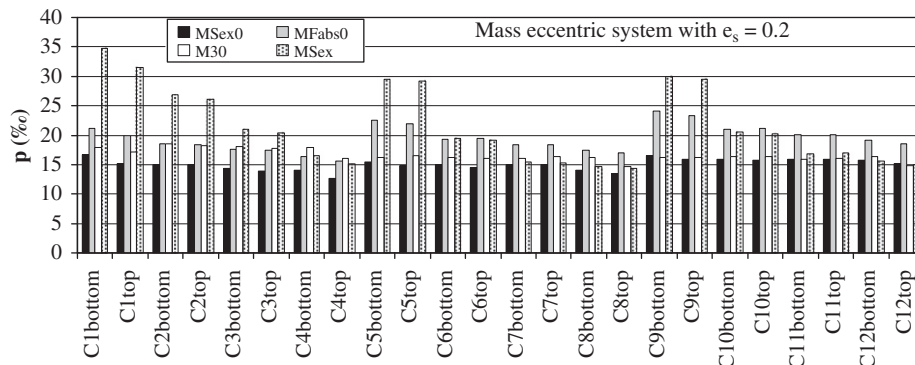


Fig. 12. Reinforcement steel ratios (p) of the columns for the mass eccentric system ($e_s=0.2$) under “San Fernando” earthquake (No. 19 of Table 6).

However, in the torsionally balanced system under “San Fernando” earthquake as well as in the mass eccentric system under both “Loma Prieta” and “San Fernando” earthquake records (Figs. 10–12), there are structural elements where the method MS_{ex} produces significantly larger reinforcement steel ratios than method MS_{ex0} . In particular, the required reinforcement steel area in columns C1 and C2 in the mass eccentric system under both “Loma Prieta” and “San Fernando” earthquake records produced by the proposed method is about twice larger than the reinforcement steel area determined by method MS_{ex0} .

Furthermore, Figs. 9–12 indicate that method MF_{abs0} produces longitudinal reinforcement steel area, which is larger than the one determined by method MS_{ex0} . A comparison between methods MF_{abs0} and MS_{ex} indicates that in the torsionally balanced system method MF_{abs0} produced larger reinforcement (Figs. 9 and 11), whereas in the mass eccentric system in many columns the reinforcement determined by the proposed method MS_{ex} is larger (Figs. 10 and 12). For example, in the mass eccentric system under “San Fernando” earthquake (Fig. 12) in columns’ sections C1, C2, C3, C5, C9 and C6 (bottom) method MS_{ex} leads to larger reinforcement steel ratios than method MF_{abs0} , while in columns C4, C7, C8, C10, C11, C12 and C6 (top) method MF_{abs0} leads to larger reinforcement. The difference between the aforementioned two methods can be significant, depending on the column section and the earthquake record. Note that in the mass eccentric system under “San Fernando” earthquake, the required reinforcement areas according to method MS_{ex} in columns C1 (top), C1 (bottom), C2 (top) and C2 (bottom) are 1.64, 1.59, 1.45 and 1.42 times larger, respectively, than the corresponding reinforcement areas determined by method MF_{abs0} (Fig. 12).

Concerning the method $M30$, the analyses failed to indicate a certain trend. In the mass eccentric system, under the “San Fernando” earthquake (Fig. 12) method $M30$ produced the largest

steel area in column C4 and the smallest steel area in column C12 (top) with regard to the other three methods.

Fig. 13 depicts the variation of the reinforcement area in column C16 (bottom) determined by the four methods presented in the paper with reference to the earthquake record. We can see that the reinforcement area is strongly depending on the earthquake record. In the torsionally balanced system, method MF_{abs0} produced the most conservative results, while in the mass eccentric system ($e_s=0.2$) method MS_{ex} was the most conservative.

In order to better quantify the differences among the results produced by the aforementioned four methods, the relative variation of method i (i : MF_{abs0} , MS_{ex0} and $M30$) with regard to the method MS_{ex} is defined as

$$RV_i = \frac{A_{s,i} - A_{s,MS_{ex}}}{A_{s,MS_{ex}}} 100(\%) \quad (9)$$

where $A_{s,i}$ or ($A_{s,MS_{ex}}$): the required reinforcement area according to the method i or (MS_{ex}).

The influence of the earthquake ground motion (soil type B) on the relative variation for column C16 (bottom) is presented in Fig. 14. As was mentioned previously, regarding the torsionally balanced system, method MF_{abs0} leads to the largest reinforcement steel ratios. However, in the mass eccentric building, the proposed method leads to the most conservative results under the vast majority of earthquake records. In this building, method MF_{abs0} produced significantly smaller reinforcement steel ratios (–34% for earthquake record No. 6 (Table 6)) than the proposed method MS_{ex} . Method $M30$ produced the smallest reinforcement in the torsionally balanced system. However in the mass eccentric model, there are earthquake ground motions (earthquake records Nos. 5 and 16), under which method $M30$ produced the most conservative results to column C16 (bottom).

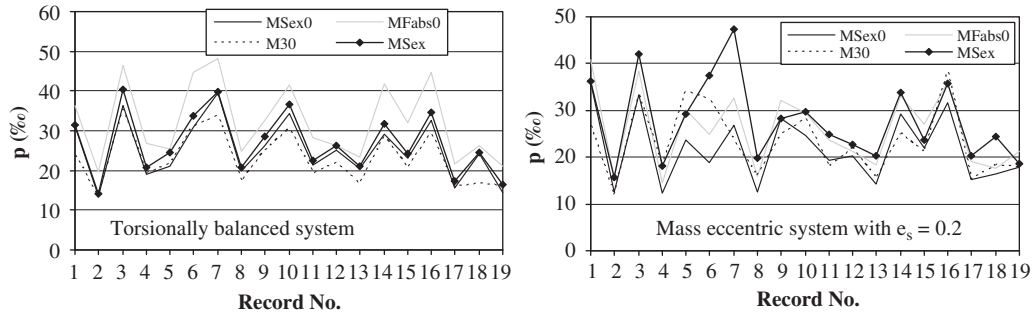


Fig. 13. Influence of the earthquake ground motion (soil type B) on the reinforcement steel ratio (p) for column C16 (bottom).

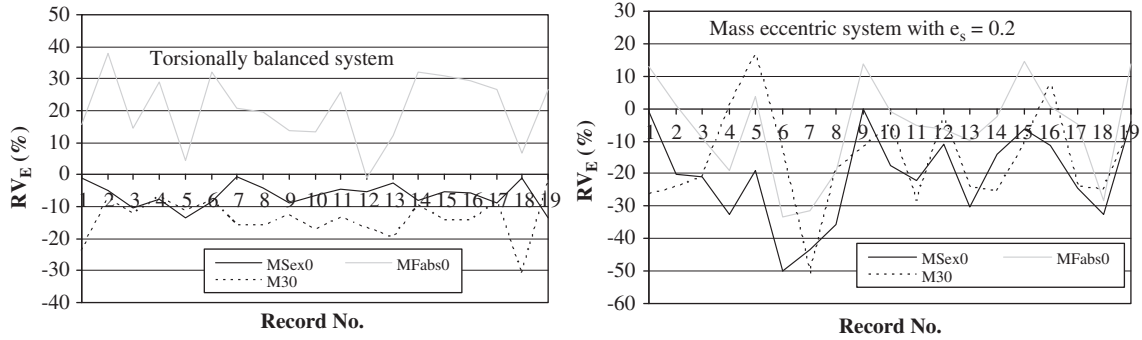


Fig. 14. Influence of the earthquake ground motion (soil type B) on the relative variation for column C16 (bottom).

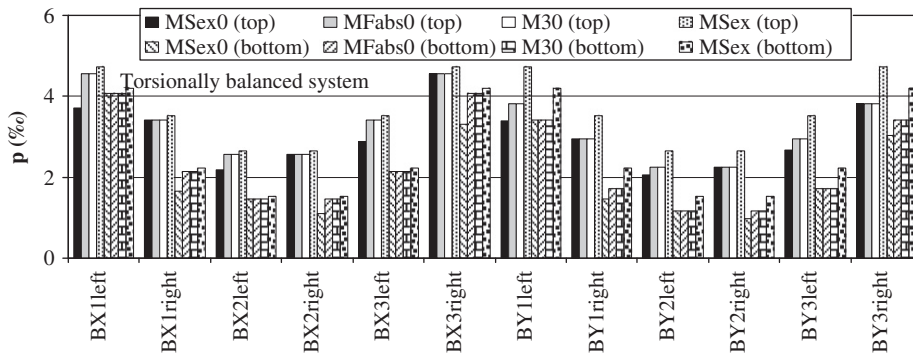


Fig. 15. Reinforcement steel ratios of the beams for the torsionally balanced system under “Loma Prieta” earthquake (No. 27 of Table 5).

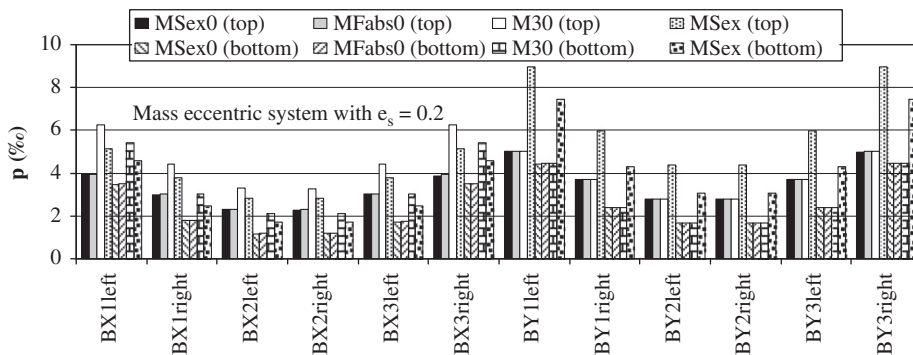


Fig. 16. Reinforcement steel ratios of the beams for the mass eccentric system ($e_s=0.2$) under “Loma Prieta” earthquake (No. 27 of Table 5).

Furthermore, the reinforcement steel ratios for every critical cross section of the beams under “Loma Prieta” earthquake records Nos. 27 and 10 (Tables 5 and 6, respectively) are presented in Figs. 15–18. We can see that the required reinforcement area is significantly affected by the method used to select the design

sectional forces. Methods MS_{ex} and MS_{ex0} produce the largest and the smallest longitudinal reinforcement steel ratios, respectively. For example, concerning the “Loma Prieta” earthquake (No. 10 of Table 6) and for the mass eccentric system (Fig. 18) the reinforcement area according to method MS_{ex} is 2.5 and 2.8 times larger than

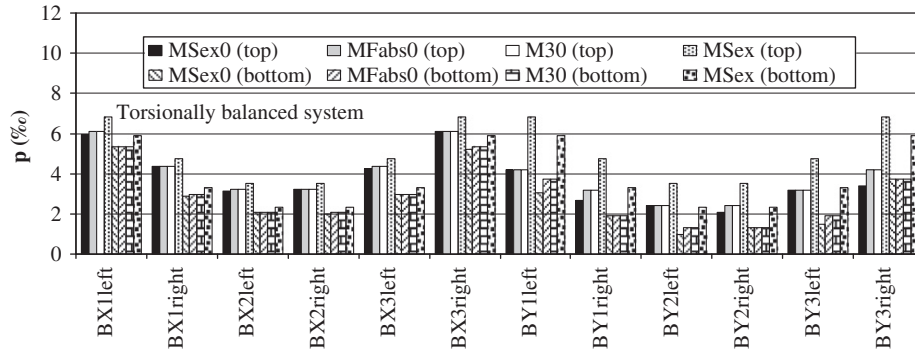


Fig. 17. Reinforcement steel ratios of the beams for the torsionally balanced system under "Loma Prieta" earthquake (No. 10 of Table 6).

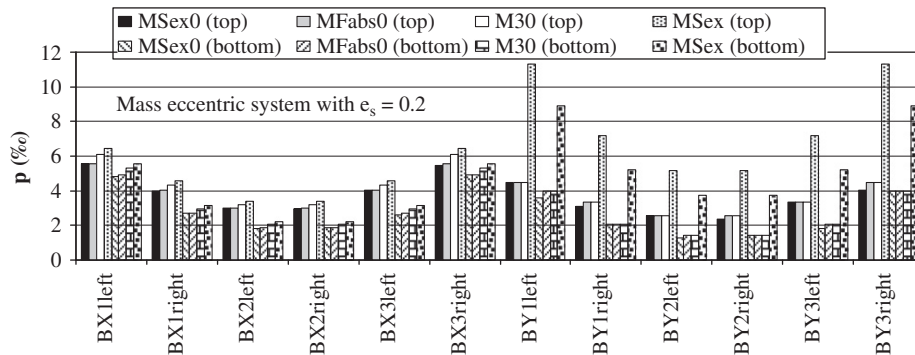


Fig. 18. Reinforcement steel ratios of the beams for the mass eccentric system ($e_s=0.2$) under "Loma Prieta" earthquake (No. 10 of Table 6).

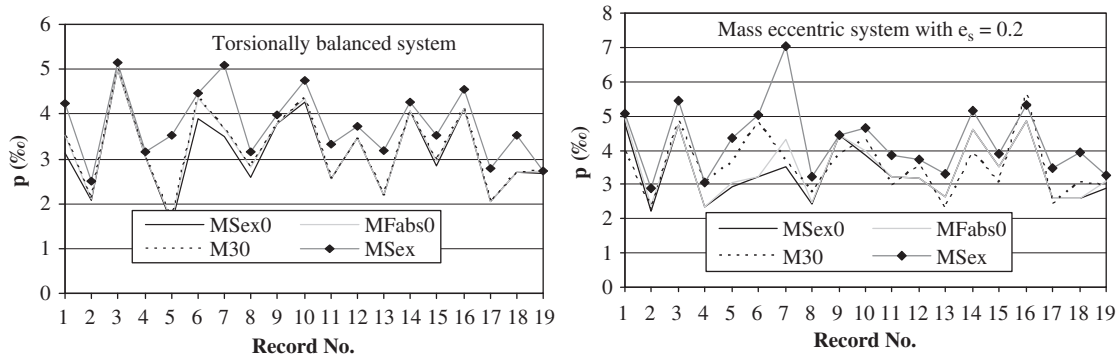


Fig. 19. Influence of the earthquake ground motion (soil type B) on the reinforcement steel ratio (p) for beam BX12top (left joint).

the reinforcement area determined by method MS_{ex0} in beams BY1top (left joint) and BY3top (right joint).

Method MF_{abs0} produced reinforcement steel ratios, which range between the reinforcement steel ratios determined by methods MS_{ex0} and MS_{ex} , while for method $M30$ no clear trend was observed.

The reinforcement steel ratio as well as the relative variation (Eq. (9)) with reference to the earthquake ground motion (soil type B) for the beam BX12top (left joint) is presented in Figs. 19 and 20. We can see that methods MF_{abs0} and MS_{ex0} , produce reinforcement steel ratios that are smaller than the ones determined by the proposed method MS_{ex} , thus underestimating seismic demands. The aforementioned underestimation can be significantly important depending on the seismic ground motion. As an example, observe that the relative variation of method MS_{ex0} (Fig. 20) can be up to -55% (Record no. 5) and -50% (Record no. 7) for the torsionally balanced and the mass eccentric system, respectively. On the other hand, there are seismic records

for which methods MS_{ex0} , MF_{abs0} and MS_{ex} produce very similar results, especially in the case of the torsionally balanced model. Concerning method $M30$, there is no clear trend. It produces smaller reinforcement ratios than the proposed method in the torsionally balanced system, while in the mass eccentric system there is only one record (No. 16, Fig. 20), for which the method $M30$ is more conservative than the proposed.

All the above results clearly indicate that the application of the seismic components along the structural axes according to code provisions can significantly underestimate seismic demands depending on the seismic input and the structural system.

7.2. Average values

The average values of the required reinforcement steel ratios corresponding to 8 representative structural elements (four columns and four beams), for all the 19 ground motions recorded

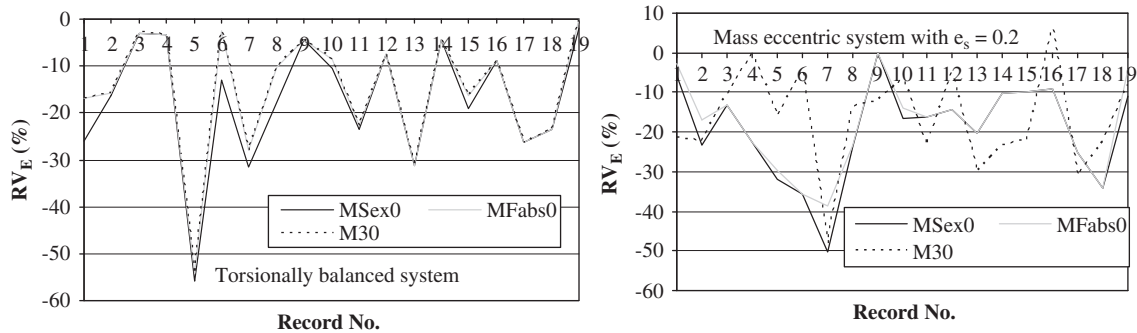


Fig. 20. Influence of the earthquake ground motion (soil type B) on the relative variation for beam BX12top (left joint).

Table 7
Average values for reinforcement steel ratios of columns C2 (top), C14 (bottom), C15 (top) and C16 (bottom) for ground motions recorded on soil type B.

		C2 (top)	C14 (bottom)	C15 (top)	C16 (bottom)
es=0	MS _{ex} 0	24.88	26.07	25.18	25.13
	MF _{abs} 0	32.28	33.27	32.28	32.18
	M30	22.82	23.41	23.41	23.01
	MS _{ex}	27.14	27.91	27.14	26.81
es=0.1	MS _{ex} 0	24.69	25.55	23.01	21.04
	MF _{abs} 0	32.00	32.77	29.26	26.52
	M30	25.79	26.21	24.59	22.85
	MS _{ex}	31.50	33.60	29.20	26.20
es=0.2	MS _{ex} 0	24.74	26.68	23.46	21.83
	MF _{abs} 0	30.77	32.19	28.47	25.89
	M30	26.17	26.53	24.81	23.18
	MS _{ex}	32.49	37.56	31.12	27.79

Table 8
Average values for reinforcement steel ratios of beams BX1top (left joint), BX4top (right joint), BY3top (right joint) and BY6top (right joint) for ground motions recorded on soil type B.

		BX1 (left)	BX4 (right)	BY3 (right)	BY6 (right)
es=0	MS _{ex} 0	4.13	3.38	3.73	3.95
	MF _{abs} 0	4.29	3.56	3.91	4.14
	M30	4.27	3.56	3.91	4.14
	MS _{ex}	5.17	4.13	5.17	5.48
es=0.1	MS _{ex} 0	4.30	3.32	4.47	3.72
	MF _{abs} 0	4.44	3.49	4.63	3.88
	M30	4.64	3.56	4.63	3.88
	MS _{ex}	5.29	4.03	6.37	5.28
es=0.2	MS _{ex} 0	4.28	3.27	4.31	3.19
	MF _{abs} 0	4.59	3.43	4.56	3.38
	M30	4.79	3.52	4.56	3.38
	MS _{ex}	5.32	3.94	6.73	5.03

on the soil type B are presented in Tables 7 and 8. It is important to notice that the trends exhibited by the columns and beams presented in Tables 7 and 8 were observed in the majority of the structural elements of the buildings studied in the present paper. In addition, the same observations are also valid for the seismic motions recorded on soil type A.

Concerning the columns, from Table 7, it is obvious that in the torsionally balanced system method MF_{abs}0 leads on an average to more conservative results than method MS_{ex}, while method MS_{ex} is more conservative with regard to both methods MS_{ex}0 and M30. However with increasing values of mass eccentricity, method MF_{abs}0 tends to underestimate the required reinforcement with respect to the method MS_{ex}. For building with e_s=0.2, methods MS_{ex}0, MF_{abs}0 and M30 underestimate the required reinforcement with regard to the proposed method. The aforementioned underestimation appears to be slightly weaker for the ground motions on the soil type A. The average values of the reinforcement steel ratios corresponding to beams (Table 8) indicate that method MS_{ex} is the most conservative, independent of the structural eccentricity.

Of particular interest is the extent to which methods MF_{abs}0, MS_{ex}0 and M30, which do not account for the orientation of the seismic input, tend to overestimate or underestimate the required longitudinal reinforcement area with regard to the proposed method MS_{ex}. Therefore, the average and minimum values (larger underestimation under a specific ground motion) of the relative variations RV (Eq. (9)) for all structural elements and ground motions used are given in Tables 9–10.

From Table 9, it is apparent that methods MS_{ex}0 and M30 underestimate the seismic demands for the columns. The underestimation appears to increase as the mass eccentricity increases for both the sets of the ground motions, although there are very few cases that method M30 produces more conservative results

Table 9
Average and minimum relative variations RV with regard to method MS_{ex} for columns.

		Soil type A			Soil type B		
		es=0	es=0.1	es=0.2	es=0	es=0.1	es=0.2
Average RV	MS _{ex} 0	-6.73	-14.78	-17.38	-7.87	-17.23	-21.30
	MF _{abs} 0	21.24	8.45	3.68	19.57	6.36	-2.09
	M30	-14.49	-16.43	-15.53	-15.35	-16.50	-19.14
Minimum RV	MS _{ex} 0	-28.29	-53.79	-62.06	-24.08	-47.29	-58.83
	MF _{abs} 0	-3.07	-32.44	-41.98	-4.24	-30.12	-50.37
	M30	-32.20	-49.83	-54.34	-35.75	-46.47	-62.38

Table 10
Average and minimum relative variations RV with regard to method MS_{ex} for beams.

		Soil type A			Soil type B		
		es=0	es=0.1	es=0.2	es=0	es=0.1	es=0.2
Average RV	MS _{ex} 0	-21.02	-20.84	-19.57	-21.34	-21.76	-22.86
	MF _{abs} 0	-17.43	-17.22	-15.48	-17.85	-18.42	-19.37
	M30	-17.42	-15.93	-14.41	-17.84	-17.05	-18.08
Minimum RV	MS _{ex} 0	-66.63	-65.55	-63.96	-72.05	-73.66	-73.29
	MF _{abs} 0	-63.41	-61.53	-61.70	-63.71	-65.99	-63.06
	M30	-63.40	-58.93	-56.24	-63.70	-64.79	-60.43

than those of method MS_{ex}, as it was shown in subSection 7.1. On the other hand, method MF_{abs}0 seems to be the most conservative for the torsionally balanced model, leading to the largest

reinforcement area in the vast majority of the columns. However with increasing values of the mass eccentricity, the reinforcement steel ratios obtained by method MF_{abs0} tend to become smaller than the ones produced by method MS_{ex} . This fact is more intense for the set of the seismic motions recorded on the soil type B (Table 9). It is interesting to notice that in the case of the soil type A, the minimum relative variation RV (maximum underestimation) reached the values of -62.06% , -41.98% and -54.34% for the methods MS_{ex0} , MF_{abs0} and $M30$, respectively. In the case of the soil type B, the minimum values of the relative variation RV are -58.83% , -50.37% and -62.38% for methods MS_{ex0} , MF_{abs0} and $M30$, respectively (Table 9).

The values of the relative variation corresponding to beams (Table 10) demonstrate that the reinforcement steel ratios produced by methods MS_{ex0} , MF_{abs0} and $M30$ are smaller than the ones determined by method MS_{ex} , regardless of the mass eccentricity or the soil type. The underestimation under a single ground motion can be up to 65.99% and 64.79% for methods MF_{abs0} and $M30$, respectively. There are very few cases that method $M30$ produced more conservative results than those obtained by method MS_{ex} , as it was shown in subSection 7.1, while method MS_{ex0} produces the smaller reinforcement ratios. The underestimation with regard to method MS_{ex} can be up to 73.66% (for the model with mass eccentricity $e_s=0.1$).

7.3. Reinforcement due to 3 or 7 earthquake records

As it was mentioned in Section 2, seismic code provisions suggest that when three time history data sets are used as seismic input, the maximum value of each response parameter must be used for design, while in the case of 7 or more time history data sets, the average value of each response parameter may be permitted to determine the design acceptability. In the following, the reinforcement determined by the application of

the individual ground motion was used as the response parameter. This choice was made because in case of using the sectional forces as response parameters, the combinations of the axial force and the two bending moments needed for the calculation of the required reinforcement in the columns would consist of sectional forces that do not necessary correspond to the same earthquake record.

In order to compare the four methods, we compute the required reinforcement areas due to 3 and 7 seismic inputs. From the analyses due to 28 (soil type A) and 19 (soil type B) earthquake ground motions, all possible combinations of 3 records are considered; for 3 out of 28 and 3 out of 19 records, there are 3276 and 969 combinations, respectively. For each one of these records combinations, the maximum value of the required reinforcement according to each one of the four methods is determined. Then, the average value of all these combinations for each method is calculated. Similarly, from the analyses due to 28 (soil type A) and 19 (soil type B) earthquake ground motions, all possible combinations of 7 records are considered; these are 1,184,040 and 50,388 combinations for soil types A and B, respectively. For each one of these combinations, the average value (corresponding to each set of 7 records) of the required reinforcement according to each one of the four methods is computed. Then, the average value corresponding to each method for all these combinations is calculated.

In Figs. 21–24, the required reinforcement steel ratios corresponding to column C15 (top) and beam BX10top (left joint) are presented. For each method, for all the above combinations of 3 as well as 7 earthquake records, the minimum value, the average value minus the standard deviation, the average value, the average value plus the standard deviation and the maximum value are plotted. It must be clarified that the maximum/minimum ratio of each method does not correspond to the same combination of 3 or 7 earthquake records.

From Figs. 21 and 22, it can be deduced that regarding the columns of the torsionally balanced model method MF_{abs0}

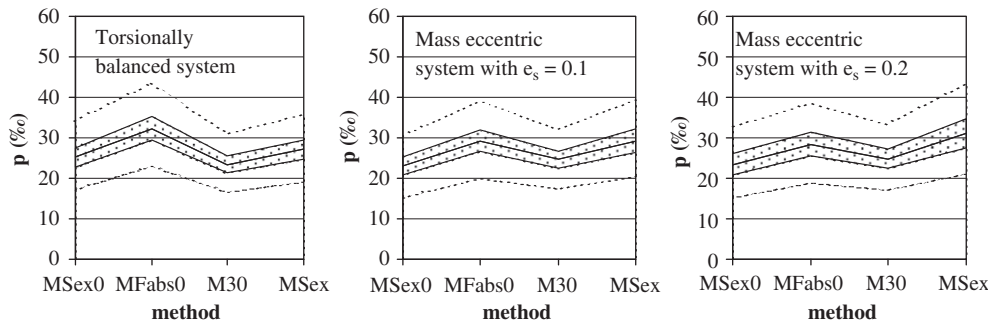


Fig. 21. Required reinforcement steel ratios in column C15 (top) according to the four methods, when 7 records (soil type B) are considered.

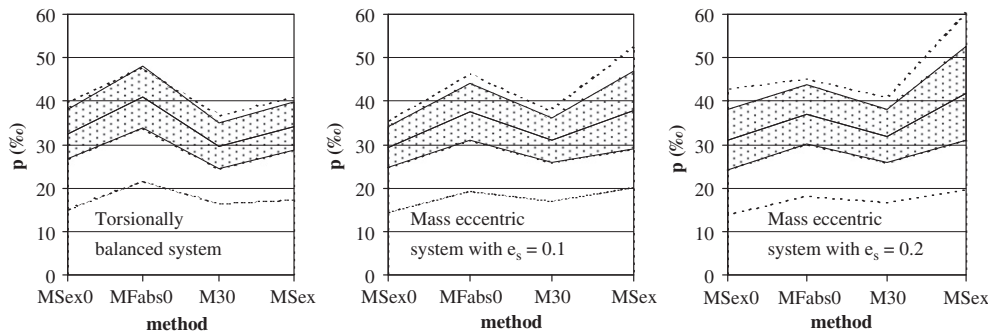


Fig. 22. Required reinforcement steel ratios corresponding to column C15 (top) according to the four methods, when 3 records (soil type B) are considered.

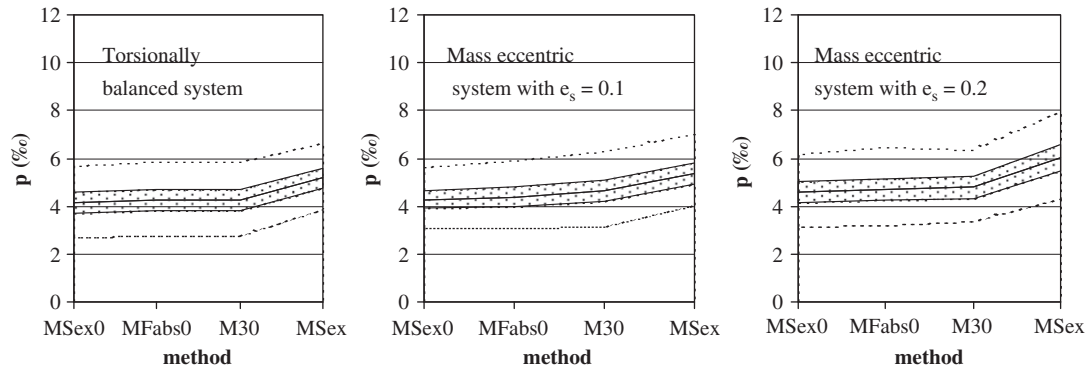


Fig. 23. Required reinforcement steel ratios corresponding to BX10top (left joint) according to the four methods when 7 records (soil type B) are considered.

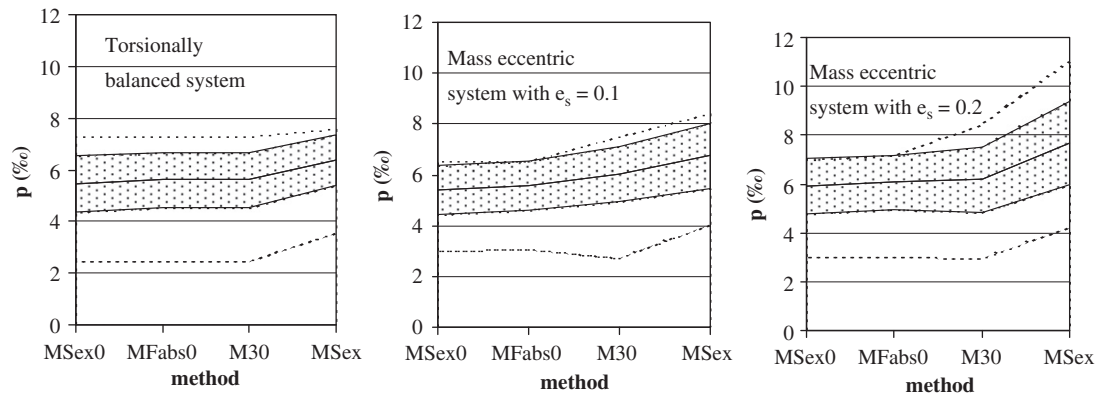


Fig. 24. Required reinforcement steel ratios corresponding to BX10top (left joint) according to the four methods, when 3 records (soil type B) are considered.

produces more conservative results than those of the proposed method MS_{ex} , whereas with increasing the mass eccentricity method MF_{abs0} tends to underestimate the reinforcement ratio with regard to method MS_{ex} . Similar results were produced for the majority of the columns due to ground motions recorded on the soil type B. Figs. 23 and 24 show that regarding the beams, methods MS_{ex0} , MF_{abs0} and $M30$ significantly underestimate the required reinforcement area with respect to the proposed method MS_{ex} . It is interesting to notice that the aforementioned observations, which are consistent with those presented in the previous subsections, are valid regardless of whether 3 or 7 records are used as seismic input.

The observations of Figs. 21 and 22 as well as Figs. 23 and 24 show that the mean value of the reinforcement ratio is smaller when seven records are used compared to the one produced by 3 records. Also, we see that when seven records are used, the mean value band-width is much narrower compared to the associated one produced by 3 records. Moreover, the standard deviation, which is a common measure of dispersion, is higher, when 3 records are used. These findings are valid for all methods of selecting the sectional forces.

8. Conclusions

In this paper, a rational procedure for the appropriate selection of the sectional forces needed for the calculation of the longitudinal reinforcement in R/C frame elements within the context of linear time history analysis is presented. The proposed method is based on the maximum normal stress occurred at a cross section for any angle of seismic incidence. Three R/C buildings (one torsionally balanced and two mass eccentric systems) are

analyzed due to 47 strong earthquake ground motions. For each ground motion, the longitudinal steel area at all critical cross sections is calculated, using the proposed method as well as three other code compatible methods. From the comparative assessment of the results, the following conclusions can be derived:

- The required reinforcement area is strongly affected by the method used to select the design sectional forces in the frame elements.
- Methods based on seismic effects produced by accelerograms applied along the structural axes can significantly underestimate the required reinforcement with respect to the proposed method MS_{ex} , depending on the mass eccentricity of the building, the kind (column or beam) and position of the structural element and the input seismic motion. The underestimation due to a single seismic motion can be up to 62.38% for the columns and 65.99% for the beams (for the studied buildings and ground motions used).
- The mean value of reinforcement underestimation with regard to the proposed method produced by methods using accelerograms applied along the structural axes due to 3 seismic records range between 5% and 25% for the columns and between 11% and 23% for the beams. The corresponding mean values of underestimation due to seven records range between 6% and 24% for the columns and between 14% and 24% for the beams. That is, the underestimation slightly depends on whether three or seven records are used as seismic input.
- Method MF_{abs0} , which uses the maximum non-simultaneous absolute values of the sectional forces produced by accelerograms applied along the structural axes, gives conservative (with regard to the proposed method) reinforcement ratios for the columns of the symmetric building, while it produces

unconservative reinforcement ratio for the beams of the same building.

Finally, it is worth mentioning that the proposed method of selecting the sectional forces (MS_{ex}) is convenient to use as it requires very little computational effort. Besides, it can be easily implemented in an existing commercial software.

References

- [1] Eurocode 8. Design of structures for earthquake resistance, Part 1: general rules, seismic actions and rules for buildings. European Committee for Standardization 2003.
- [2] NEHRP (FEMA 450). Recommended provisions for seismic regulations for new buildings and other structures. Part 1—Provisions, Federal Emergency Management Agency, Washington, DC 2003.
- [3] FEMA 356. Prestandard and commentary for the seismic rehabilitation of buildings. Federal Emergency Management Agency, Washington, DC 2000.
- [4] ASCE 41/06. Seismic rehabilitation of existing buildings, American Society of Civil Engineers 2009.
- [5] EAK 2003. Greek code for earthquake resistant design of structures. Ministry of Environment, Planning and Public Works. Greece 2003.
- [6] Smeby W, Der Kiureghian A. Modal combination rules for multi-component earthquake excitation. *Earthquake Eng Struct Dyn* 1985;13:1–12.
- [7] Anastassiadis K. Directions sismiques défavorables et combinaisons défavorables des efforts. *Ann IT B T P* 1993;512:83–99.
- [8] Lopez OA, Torres R. The critical angle of seismic incidence and the maximum structural response. *Earthquake Eng Struct Dyn* 1997;26:881–94.
- [9] Menun C, Der Kiureghian A. A replacement for the 30%, 40% and SRSS rules for multicomponent seismic analysis. *Earthquake Spectra* 1998;14(1):153–63.
- [10] Lopez OA, Chopra AK, Hernandez JJ. Critical response of structures to multicomponent earthquake excitation. *Earthquake Eng Struct Dyn* 2000;29:1759–78.
- [11] Menun C, Der Kiureghian A. Envelopes for seismic response vectors. I: theory. *J Struct Eng* 2000;126:467–73.
- [12] Menun C, Der Kiureghian A. Envelopes for seismic response vectors. II: application. *J Struct Eng* 2000;126:474–81.
- [13] Lopez OA, Chopra AK, Hernandez JJ. Evaluation of combination rules for maximum response calculation in multicomponent seismic analysis. *Earthquake Eng Struct Dyn* 2001;30:1379–98.
- [14] Anastassiadis K, Avramidis I, Panetos P. Concurrent design forces in structures under three-component orthotropic seismic excitation. *Earthquake Spectra* 2002;18:1–17.
- [15] Fernandez-Davila I, Cominetti S, Cruz E.F. Considering the bi-directional effects and the seismic angle variations in building design. In: *Proc 12th World Conf Earthquake Eng. Auckland, New Zealand: Paper No.435* 2000.
- [16] Athanatopoulou AM. Critical orientation of three correlated seismic components. *Eng Struct* 2005;27:301–12.
- [17] Athanatopoulou AM, Tsourekas A, Papamanolis G. Variation of response with incident angle under two horizontal correlated seismic components. In: *Proc Earthquake Resistant Eng Struct V. (Skiathos, Greece): 2005*. p. 183–192.
- [18] Athanatopoulou AM, Avramidis IE. Effects of seismic directivity on structural response. In: *Proc Second Fib Congr. (Naples, Italy): paper ID 8–15* 2006.
- [19] Gupta AK, Singh MP. Design of column sections subjected to three components of earthquake. *Nucl Eng Des* 1977;41:129–33.
- [20] FEMA 440. Improvement of nonlinear static seismic analysis procedures, Federal Emergency Management Agency, Washington, DC, 2004.
- [21] Pacific Earthquake Engineering Research Center (PEER). Strong Motion Database. <<http://peer.berkeley.edu/smcat/>>, 2003.
- [22] CSI. Sap2000: V11.0—integrated software for structural analysis and design. Berkeley, CA, USA: Computer and Structures Inc. (CSI); August 2004.
- [23] EKOS 2000. Greek code for the design and construction of concrete works. Greek Ministry of Environment, Planning and Public Works. (Greece): 2000.
- [24] CEN 1991. Eurocode 2: design of concrete structures. 1: general rule and rules for buildings. ENV 1992-1-1. (Brussels): 1991.
- [25] CEB-FIP. CEB-FIP model code 1990. CEB Bulletin d'Information No. 203-204-205. (Lausanne, Switzerland): 1991.
- [26] CEB-FIP. CEB-FIP manual on bending and compression—design of sections under axial action effects at the ultimate limit state. CEB Bulletin d'Information no. 141. (Lausanne, Switzerland): 1982.